Rev. Adv. Mater. Sci. 45 (2016) 36-41

MOLECULAR DYNAMICS SIMULATION STUDY OF THERMAL CONDUCTIVITIES FOR TWISTED AND UNTWISTED SINGLE-WALLED CARBON NANOTUBES

S. Saha[1] and K. Talukdar[2]

[1]Carbon Nanotechnology Group, Department of Physics, National Institute of Technology Durgapur-713209, West Bengal, India

[2]Department of Physics, Nadiha High School, Durgapur-713218, West Bengal, India

Received: January 13, 2016

Abstract. Phonons are the main carriers of heat in materials and they play a major role in the thermal behavior of the material in the nanoscale regime. In this study, we have investigated how vibrational energy of phonons is changed during the heat flow through carbon nanotubes. The variation of phonon energy of an armchair (7,7), zigzag (10,0), and chiral (6,3) single-walled carbon nanotubes (SWCNTs) for radial breathing (symmetric stretching) and torsional modes is investigated keeping their length fixed. We varied the annealing temperature from 100K to 800K gradually and studied the conformational change of the CNTs by molecular dynamics simulation. We have also estimated the thermal conductivity of the CNTs by Fourier law using non-equilibrium heat transfer approach. For the radial breathing mode, the energy peaks are observed in a wide range of frequency spectrum but for the torsional mode the peaks are shifted by small amount. In our calculation, maximum thermal conductivity is observed for the armchair CNT. Estimation of thermal conductivity of the SWCNTs at different twisting angles is performed to have an idea of the role of chirality on the thermal conductivity.

1. INTRODUCTION

Carbon nanotubes (CNTs) are considered as main building blocks in modern miniaturization technology due to their excellent electronic, thermal and mechanical properties. The heat dissipation issue is the most important factor while fabricating nanoscale electronic devices. So, study of the detailed thermal properties of the building materials is necessary for effective design of field-emitting electronic devices [1,2,3], sensors [4], thin-film transistors [5] etc. In the past few years investigations [6-9] regarding the thermal conductivities of CNTs have been performed, the outcome of which points towards high thermal conductivity of these materials. The values found by MD simulation range from 40 – 6600 W/mK. Some recent theoretical studies have explored some unknown facts like chirality effects on phonon spectra [10], thermal properties of defective graphene [11], polaron effects on thermal conductivity of zigzag CNTs [12] and thermal properties of CNT composites [13], etc. All the investigators found a dependence of thermal conductivity of the CNTs on their lengths. Both equilibrium and non-equilibrium heat transport approaches are reported [14] in various literature. In spite of so many research approaches, experimental values of thermal conductivity are largely different from that of the theoretical values. Also theoretical as well as ex-

Corresponding author: S. Saha, e-mail: saikat.meindia@gmail.com

perimental values show a wide range [15-17] variation.

Motivated by the need of a comprehensive investigation of the dependence of thermal conductivity on tube length and chirality and a huge difference of values of thermal conductivity still obtained, the present study is taken up. Here, firstly we have calculated the variation of phonon energy with respect to the vibrational frequency at different temperatures for different chiralities of the CNTs for radial breathing and torsional mode of vibration. Secondly, the thermal conductivities of different types of CNTs have been calculated keeping their length fixed. Dependence of thermal conductivity on the temperature and length is investigated. Thirdly, the thermal conductivity of the SWCNTs is found with varying twisting angles.

2. MODELING METHODOLOGY

We have performed molecular dynamics simulation to find phonon energy with frequency using Tersoff potential [18] and in the second part calculated thermal conductivity of three different types of CNTs using modified Morse (MM) potential [19]. Here thermal conductivity of individual CNT is evaluated following non-equilibrium MD. First, constant temperature simulation (NVT) is run for minimum of 100000 steps and then temperature difference is applied between the two ends of the tubes. For calculation of thermal conductivity, the average of the temperatures of hot and cold reservoirs is taken. For the remaining portion constant energy simulation (NVE) is performed. The heat flux is constant through out the sample tubes. In all these investigations, relaxation time is fixed as 0.1 fs and time for each step of simulation is 0.3 fs. As MM inter-atomic potential function can well described the behavior of atomic interactions in CNTs and also describe the creation and destruction of bonds on the application of external forces, we have used this potential in this part of our work. Thermal conductivity k is calculated using the one-dimensional form of Fourier law,

$$Q = -kA\frac{\mathrm{d}T}{\mathrm{d}x}, \tag{1}$$

Here dT/dx is the established temperature gradient and A is the cross-sectional area of the tube. Temperature is calculated by the formula

$$T = \frac{2}{Nk_B}\sum_i \frac{p_i^2}{m_i}, \tag{2}$$

where T is the average temperature, N is the number of carbon atoms, k_B is the Boltzman's constant and m_i and p_i are the atomic mass and momentum of the i-th atom respectively. By finding dT/dx, thermal conductivity can be calculated. Periodic boundary conditions are applied to avoid finite length effect. Tersoff potential has been incorporated to get the time evolution of phonon energies among the vibrational modes of the CNTs. The energy dissipation process within nano-scale structures is observed by plotting vibrational energy through the modes of the systems as a non-equilibrium population of phonons dissipating towards thermal equilibrium. Only single vibrational mode at a time is taken. Phonon energy is calculated for 30000 MD steps with time step of 0.5 fs.

3. POTENTIAL FUNCTIONS USED

Two potential energy functions are used in this work of which MM potential is employed in the conductivity measurement. The potential contains two parts; bond-stretching component E_s and angle-bending component E_b.

$$E = E_s + E_b, \tag{3}$$

where E_s and E_b are given as

$$E_s = D_e\left(\left[1-\exp^{-\beta(r-r_0)}\right]^2 - 1\right), \tag{4}$$

$$E_b = \frac{1}{2}k_\theta\left(\theta-\theta_0\right)^2\left[1+k_{sextic}\left(\theta-\theta_0\right)^4\right], \tag{5}$$

where r is the interatomic distance, θ is the angle of the adjacent bond, D_e is the dissociation energy and β is a constant related to the width of the potential.

The form of the Tersoff potential is

$$E = \sum E_i = \frac{1}{2}\sum_i\sum_{i\neq j} V(r_{ij}), \tag{6}$$

where,

$$V(r_{ij}) = f_c(r_{ij})\left[V^R(r_{ij}) + b_{ij}V^A(r_{ij})\right]. \tag{7}$$

Here E is the total energy and is decomposed into a site energy E_i which is a function of bond energy $V(r_{ij})$, where $f_c(r_{ij})$ is a cut-off function that reduces to zero interaction beyond 2.0 Å. $V^R(r_{ij})$ is a pairwise term that models the core-core and electron-electron repulsive interactions and $V^A(r_{ij})$ is a pairwise term that models core-electron attractive interactions, where r_{ij} is the distance between nearest neighbor atoms i and j, and b_{ij} is a many-body, bond-order term that depends on the number and types of neighbors and the bond angles.

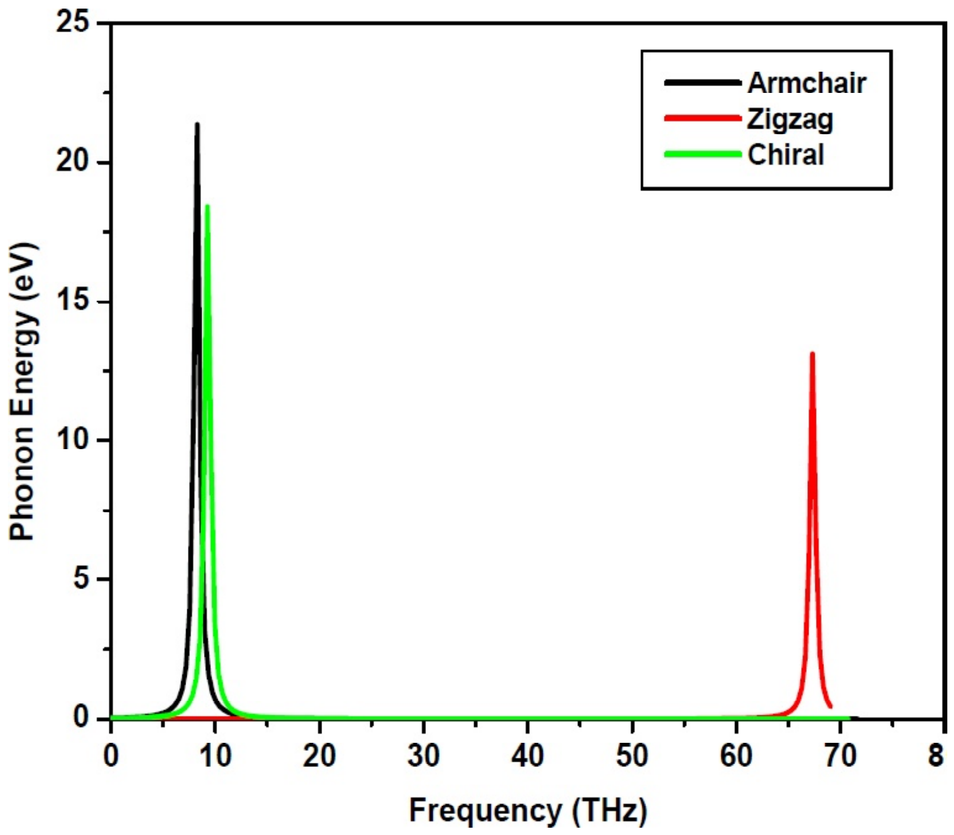

Fig .1. Frequency vs. phonon energy curve at 300K for different types of CNTs in radial breathing mode (stretching).

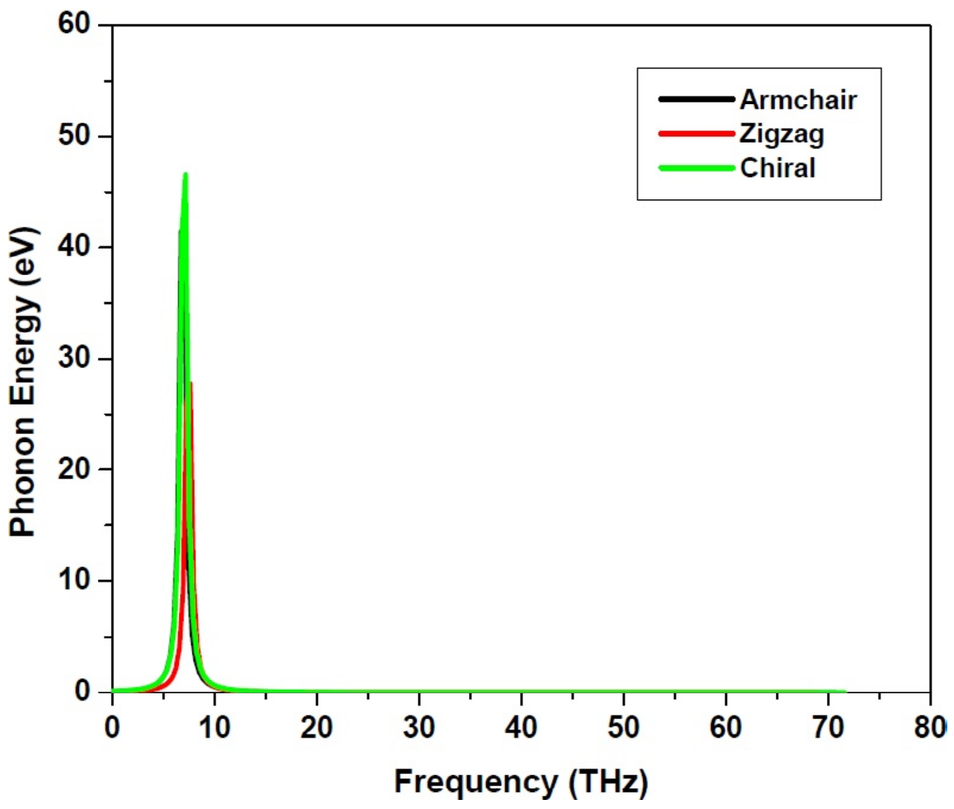

Fig. 2. Frequency vs. phonon energy curve at 800K for different types of CNTs in torsional mode.

4. RESULTS AND DISCUSSION

4.1. Phonon energy spectrum

Carbon nanotubes, due to their excellent thermal, mechanical and electronic properties are potential candidates for many thermo-electric applications. Phonon-phonon and electron-phonon scattering play important role in carrier transport of CNTs [20,21]. In different energy regimes the phonon energies are different at a constant temperature. High phonon energy indicates less thermally populated phonons which in turn indicate high mobility in CNTs at a particular temperature. We have found the phonon energy of (7,7), (10,0), and (6,3) CNTs with respect to frequency. The variation of phonon energy with frequency for radial breathing (stretching) mode at 300K and torsional mode at 800K is shown in Figs.

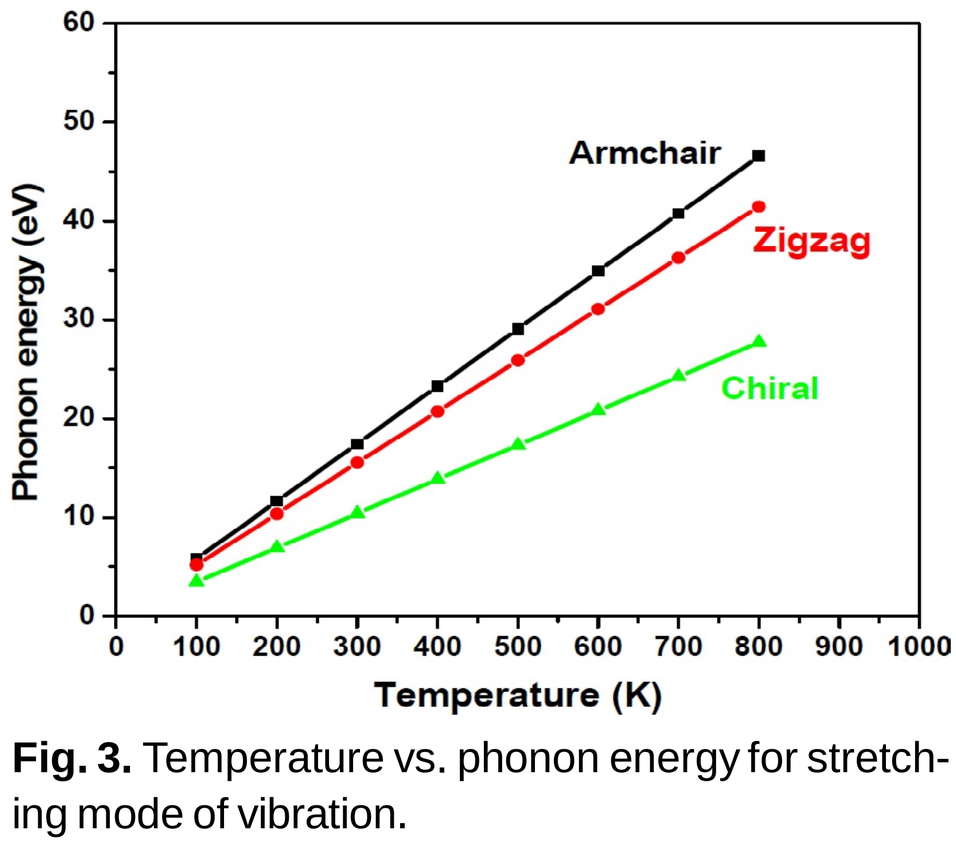

Fig. 3. Temperature vs. phonon energy for stretching mode of vibration.

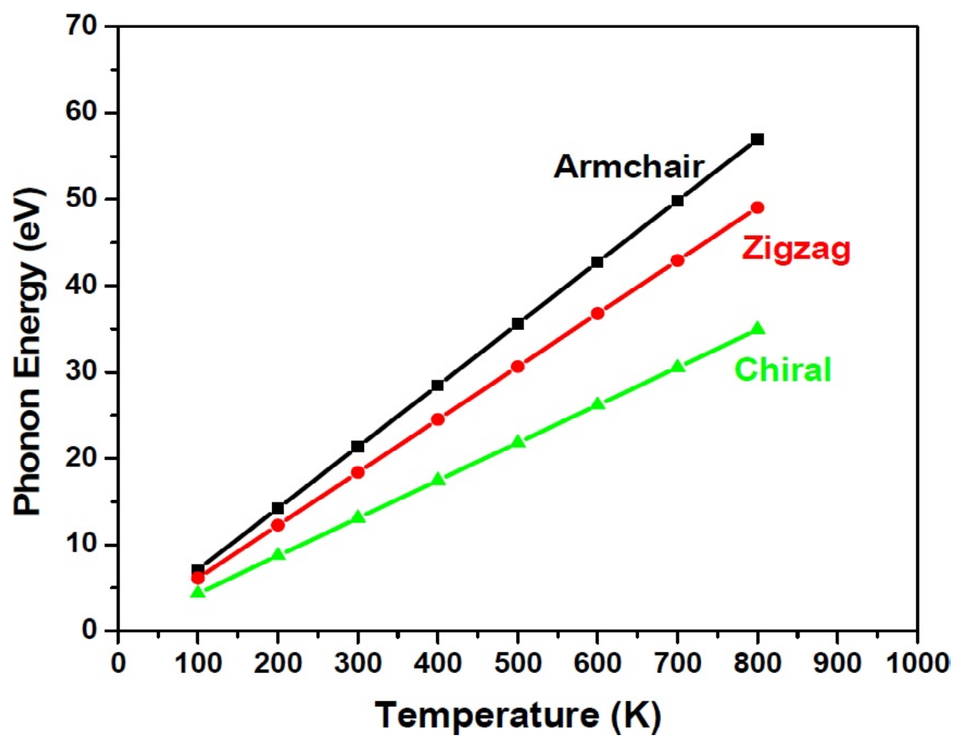

Fig. 4. Temperature vs. phonon energy for torsional mode of vibration.

1 and 2, respectively. The room temperature behavior (Fig. 1) shows high mobility of carriers for armchair CNT in radial breathing mode where for zigzag tube low energy peak for higher frequency is observed, showing somewhat different energy dissipation process. At the same temperature torsional mode shows more or less similar energy spectra for the three different tubes. With the increase of temperature, phonon energy increases linearly for both the two modes. To compare the energy spectra the length of the CNTs are taken same as 25 Å in calculating the phonon energy at different temperatures. Figs. 3 and 4 show the variation of phonon energy with temperature for the three different tubes in two modes of phonon vibration.

4.2. Thermal conductivity of untwisted SWCNTs

Using MM potential thermal conductivities of the three CNTs are calculated. The time variation of thermal conductivity of (7, 7), (10,0), and (6,3) CNTs at tem-

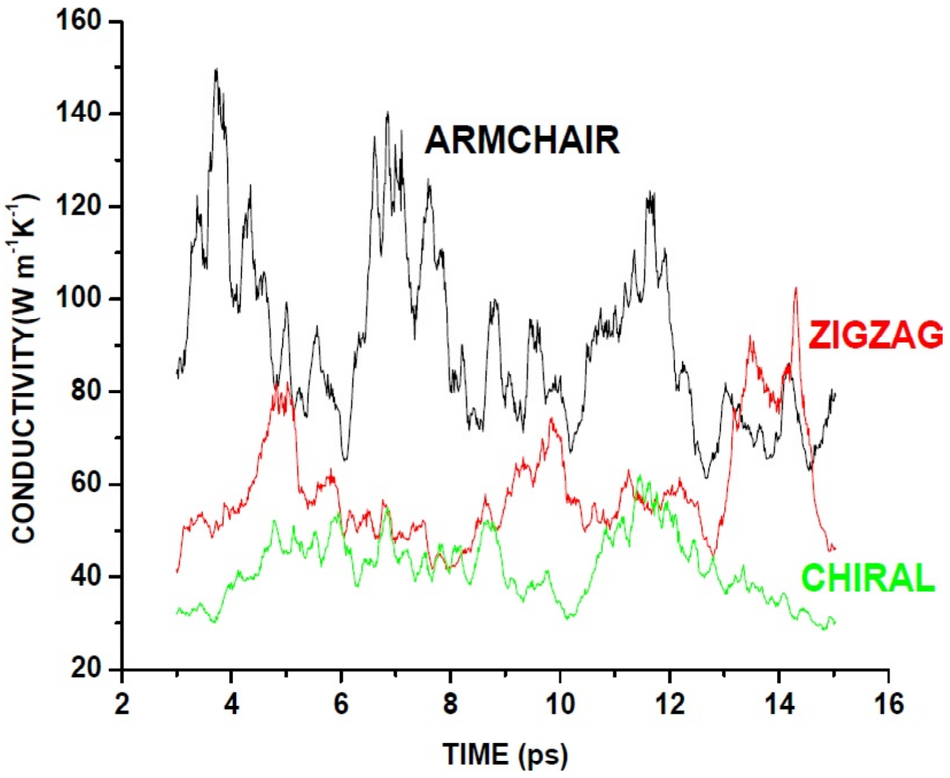

Fig. 5. Conductivity variation with time step for three different types of SWCNTs.

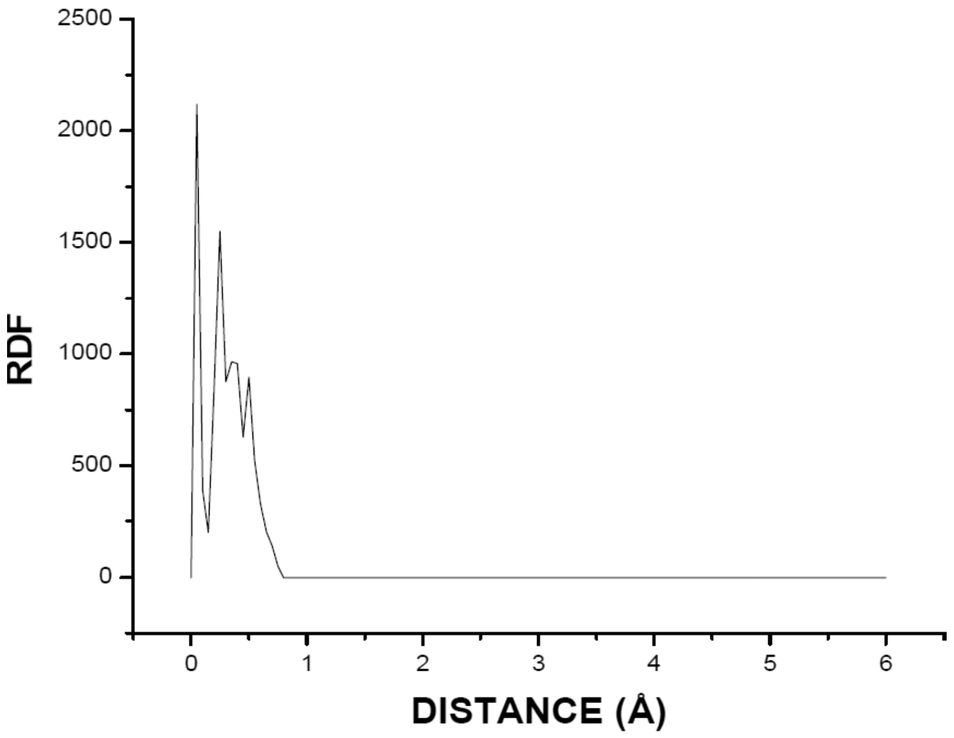

Fig. 6. RDF vs. distance for a (10,0) SWCNT.

perature 300K is shown in Fig. 5. Fig. 6 depicts the radial distribution function (RDF) for the three CNTs at 300K. In studying thermal properties of the CNTs, the phonon-phonon interaction is an important factor which is the reason of thermal resistance. The well known Umklapp process (U-process) [22,23] is the governing process of thermal resistance inside the CNTs. In our study the diameters of (6,3), (10,0), (7,7) tube are 6.214 Å, 7.774 Å, and 9.492 Å, respectively. The (7,7) tube being of highest diameter its radial and azumuthal components of the wave factor are less dominant like the narrowest (6,3) tube. So, three phonon U-process is dominant in (6,3) tube than that of (7,7) tube. Also, the armchair symmetry is such that the excess strain produced due to heat flow along the circumference of the armchair nanotube can't limit the mean free path due to the scattering like a chiral nanotube. The thermal conductivity of the materials where the phonon interaction is dominant is given by Eq. (1). So the chiral nanotube has lowest thermal conductivity while the armchair tube shows the highest value.

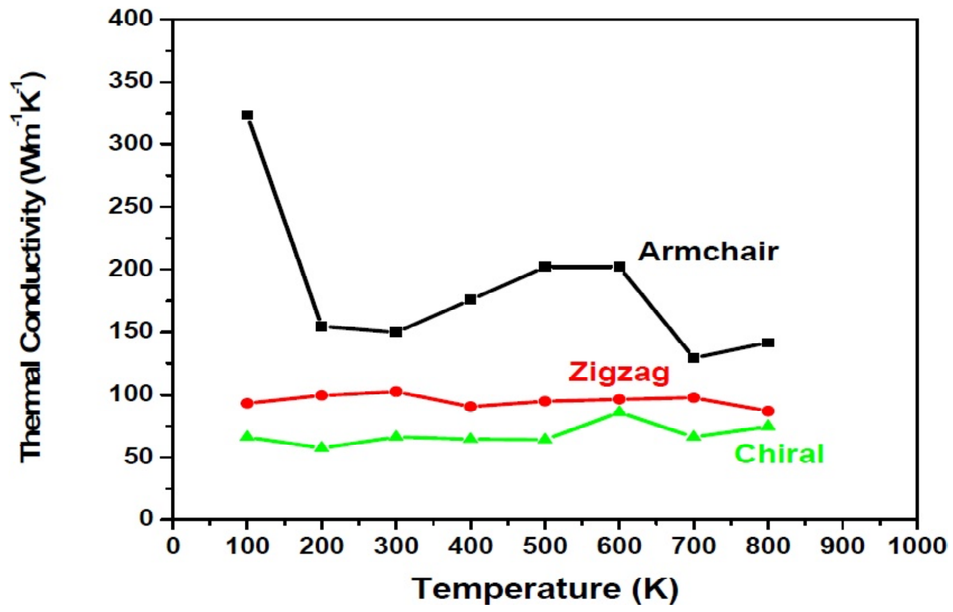

Fig. 7. Temperature vs. thermal conductivity for different types of SWCNTs.

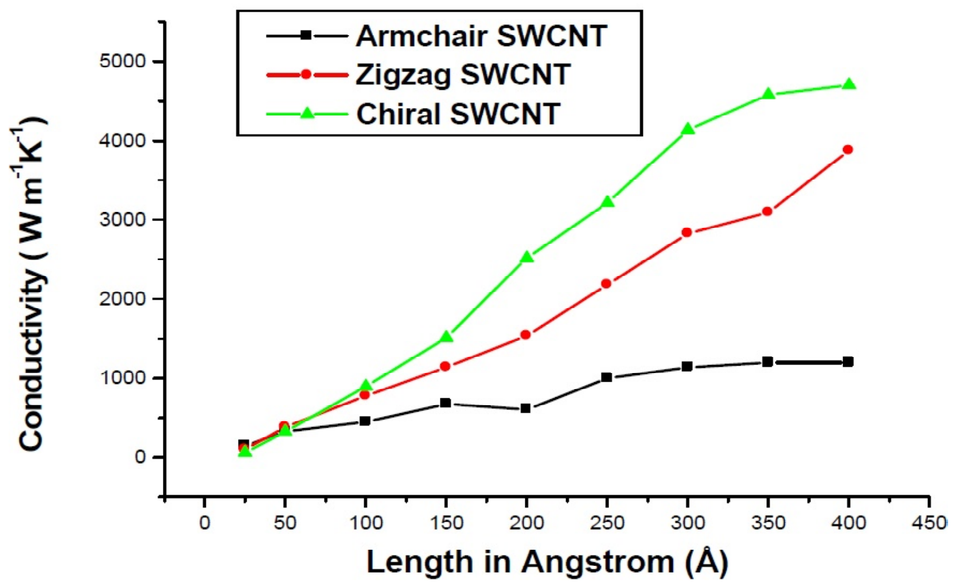

Fig. 8. Length vs. thermal conductivity for different types of SWCNTs.

We have also plotted the variation of thermal conductivities with respect to temperature which is shown in Fig. 7. All the tubes are of same length as 25 Å. The variation is most prominent for the armchair tube and only a little variation is observed for the zigzag tube. The change of thermal conductivity with length of the SWCNTs is plotted in Fig. 8. Unlike the zigzag and chiral SWCNTs, the armchair SWCNT comparatively vary a little with length, though it has largest diameter among the three tubes. Maximum variation is observed for chiral tube. The variation of conductivity with length of the CNT is given by Eq. (9). Eqs. (10) and (11) show the nature of variation of thermal conductivity of the (10,0) and (6,3) SWCNTs.

$$\Lambda_1 = A_1 + A_2 l - A_3 l^2, \tag{9}$$

$$\Lambda_1 = -B_1 + B_2 l + B_3 l^2, \tag{10}$$

$$\Lambda_1 = -C_1 + C_2 l - C_3 l^2, \tag{11}$$

where l is the thermal conductivity and *l* is the length of the tube.

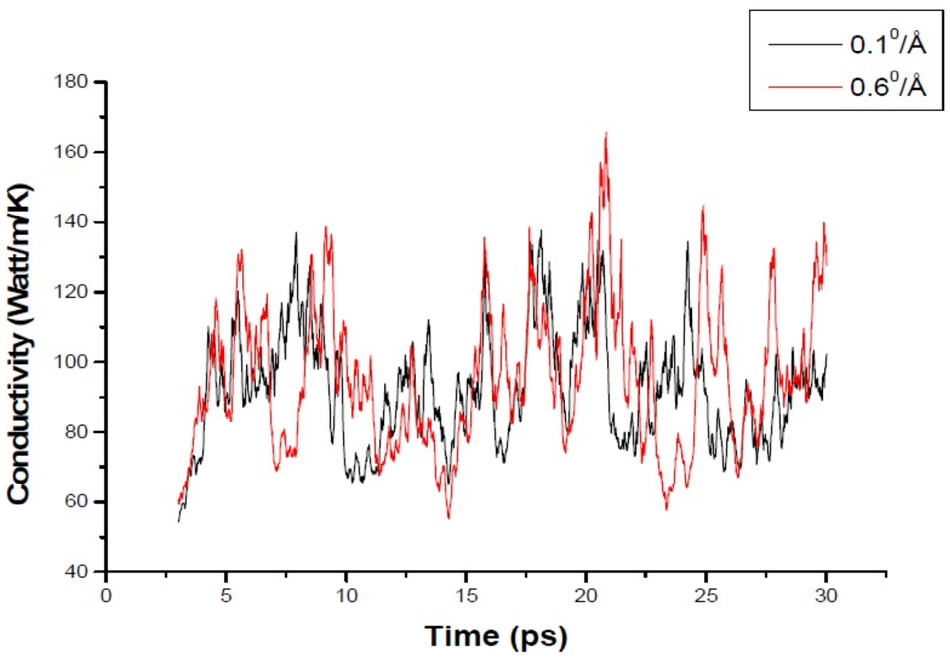

Fig. 9. Thermal conductivity of a twisted zigzag SWCNT at two different twisting angles.

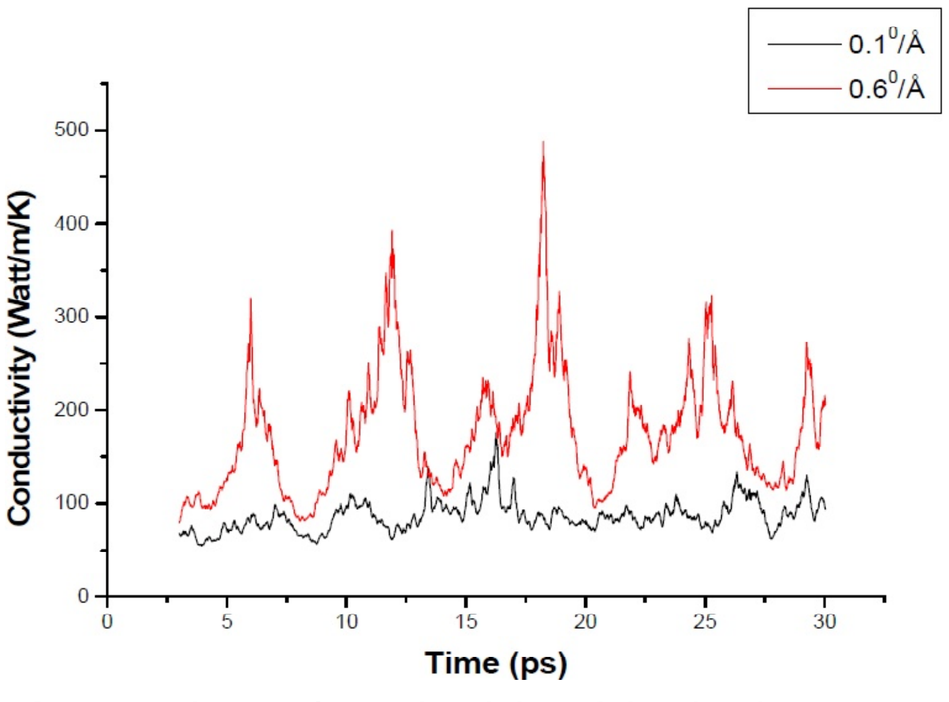

Fig. 10. Thermal conductivity of the (6,3) SWCNT at two different twisting angles.

In the above three equations, the third term is very small and of the order of 10^{-3}. So, neglecting the third term, the chiral and zigzag tubes show the same kind of variation of thermal conductivity with length. The chiral tube shows maximum variation of thermal conductivity with length and maximum value of that physical quantity at all lengths compared to the other tubes.

4.3. Thermal conductivity of twisted SWCNTs

Twisted CNTs exhibit surprisingly high thermal conductivity and their conductivity increases with the twisting angle. The conductivity of the twisted zigzag tube is least among all. The variation of thermal conductivity with twisting angle shows two different patterns; one set of values for twisting angle of 0-0.3°/Å and other set is for 0.4-0.6°/Å [Figs. 9 and 10] for zigzag and chiral SWCNTs. For armchair SWCNT the same variation of thermal conductivity is observed for all twisting angles [Fig. 11]. The values of thermal conductivity of the SWCNTs for length of 50 Å are tabulated in Table 1. For the twisted

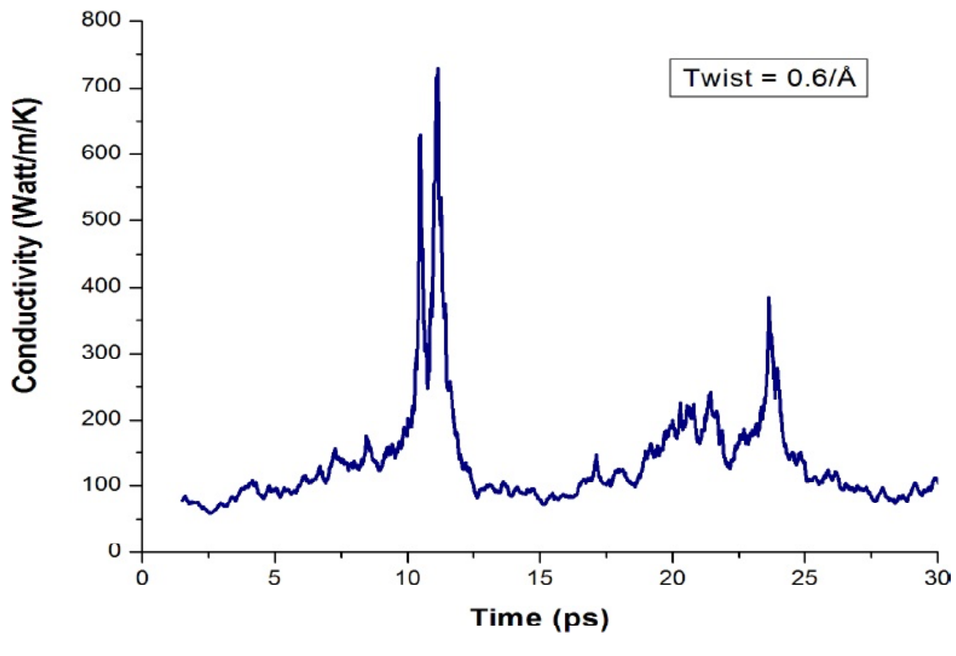

Fig. 11. Thermal conductivity of an armchair SWCNT at twisting angle 0.6°/Å.

tubes, the highest values of the thermal conductivity are tabulated. Comparing with the thermal conductivity of the untwisted chiral SWCNTs, here it is observed that with the increase of twisting angle, conductivity increases for all three types of SWCNTs. It can be inferred that either the chiral tubes or the tubes which have changed chiral indices due to twisting have greater thermal conductivity. As the armchair symmetry is changed due to torsional strain, they also exhibit higher thermal conductivity like the untwisted chiral tube.

5. CONCLUSIONS

By homogeneous non-equilibrium method using modified Morse potential thermal conductivity of single walled carbon nanotubes is calculated which shows maximum conductivity for the largest diameter armchair tube and lowest conductivity for smallest diameter chiral tube. Large variation of thermal conductivity on temperature is observed for armchair tube, while the same tube shows only a little variation of conductivity with length. Among the three tubes, the conductivity varies a lot with length. Phonon energy variation for different chirality tubes gives the phonon-phonon interaction at different temperatures. High carrier mobility in CNTs is also

Table 1. Thermal conductivity of the untwisted and twisted SWCNTs of length 50 Å.

	Thermal conductivity ($Wm^{-1} K^{-1}$)		
	Zigzag SWCNT	Chiral SWCNT	Armchair SWCNT
Untwisted SWCNT	132.3	345.2	349.5
Twisted SWCNT	161.1	487.9	728.9

proved. Twisted SWCNTs show higher thermal conductivity than that of the untwisted tubes.

REFERENCES

[1] W. A.deHeer, A.Châtelain and D.Ugarte // *Science* **270** (1995) 1179.

[2] A.G.Rinzle, J.H.Hafner,P.Nikkolaev, L.Lou,S.G.Kim, D.Tomanek, P.Nordlander, D.T.Colbert and R.E.Smalley // *Science* **269** (1995) 1150.

[3] A. V. Eletskii // *Phys. –Usp* **53** (2010) 863.

[4] R. H. Baughman, A. A. Zakhidov and W. A. de Heer // *Science* **297** (2002) 787.

[5] R.S. Ruoff and D. C. Lorents // *Carbon* **33** (1995) 925.

[6] M. Seiner, M. Freitag, V. Perebenios, J. C. Tsang, J.P. Small, M. Kinoshita, D. Yuan, J. Lie and P. Avouris // *Nature Nanotechnology* **4** (2009) 320.

[7] X. Huang, J. Wang, G. Ere and X. Wang // *Carbon* **49** (2011) 1680.

[8] A. N. Imtani // *Journal of Physics and Chemistry of Solids* **74** (2013) 1599.

[9] A. Saeedi, F.Y. Akizi, S. Khademsadr, M.E. Foulaadvand // *Solid State Communications* **179** (2014) 54.

[10] N.G. Mensah, G. Nkrumah, S.Y. Mensah and F.K.A. Allotey // *Physics Letters A* **329** (2004) 369.

[11] B. Mortazavi and A. Ahzi // *Carbon* **63** (2013) 460.

[12] H. Rezania and F. Taherkhani // *Solid State Communications* **152** (2012) 1776.

[13] S. Wang, R. Liang and C. Zhang // *Carbon* **47** (2009) 53.

[14] J.A. Thomas, J.E.Turney, R.M.Iutzi, C.H. Amon and A.J.H. McGaughey // *Phys. Rev. B* **81** (2010) 091411(R).

[15] P. Kim, L. Shi, A. Majumdar and P.L. McEuen // *Phys. Rev. Lett.* **87** (2001) 215502.

[16] M. Fujii, X. Zhang, H. Xie, H. Ago, K. Takahashi and T. Ikuta // *Phys. Rev. Lett.* **95** (2005) 065502.

[17] T. Y. Choi, D. Poulikakos, J. Tharian and U. Sennhauser // *Nano Lett.* **6** (2006) 1589.

[18] J. Tersoff // *Phys. Rev. Lette*r **61** (1988) 2879.

[19] L. Cheng and J. Yang // *The Journal of Chemical Physics* **127** (2007) 124104.

[20] M.S. Dreesselhaus and P.C. Eklund // *Adv. Phys.* **49** (2000) 705.

[21] T. Yamamoto, S. Watanabe and K. Watanabe // *Phys. Rev. Lett.* **20** (2004) 075502.

[22] Y. Xiao, X. H. Han, J.X. Cao and J. W. Ding // *Journal of Physics: Condensed Matter* **15** (2003) L341.

[23] Y.Gu and Y. Chen // *Physical Review B* **76** (2007) 134110.